Arabian Journal of Chemistry (2023) **16**, 104604

King Saud University

Arabian Journal of Chemistry

www.ksu.edu.sa
www.sciencedirect.com

ORIGINAL ARTICLE

Hibiscus sabdariffa synthesized gold nanoparticles ameliorate aluminum chloride induced memory deficits through inhibition of COX-2/BACE-1 mRNA expression in rats

Scholastica O. Anadozie [a,*], Duncan O. Effiom [a], Olusola B. Adewale [a], Jodie Jude [a], Itumeleng Zosela [b], Oluwole B. Akawa [c,d], Juliet N. Olayinka [e], Saartjie Roux [b]

[a] *Biochemistry Program, Department of Chemical Sciences, Afe Babalola University, P.M.B 5454, Ado-Ekiti, Nigeria*
[b] *Department of Human Physiology, Nelson Mandela University, P.O Box 77000, Port Elizabeth, South Africa*
[c] *Department of Pharmacology and Toxicology, College of Pharmacy, Afe Babalola University, P.M.B 5454, Ado-Ekiti, Nigeria*
[d] *Molecular Biocomputation and Drug Design Laboratory, School of Health Sciences, University of KwaZulu-Natal, Westville Campus, Durban 4001, South Africa*
[e] *Department of Pharmacology and Therapeutics, College of Medicine and Health Sciences, Afe Babalola University, P.M.B 5454, Ado-Ekiti, Nigeria*

Received 1 November 2022; accepted 15 January 2023
Available online 23 January 2023

KEYWORDS

Aluminum chloride;
Alzheimer's disease;
Cyclooxygenase-2;
Hibiscus sabdariffa;
Gold nanoparticle

Abstract Alzheimer's disease (AD) is a major health challenge worldwide, especially among the elderly. The disease is associated with cognitive and memory deficits. This study investigated the effect of *Hibiscus sabdariffa* synthesized-gold nanoparticles (HS-AuNPs) on $AlCl_3$-induced memory deficits in rats. Forty-two male Wistar rats were divided into six groups (n = 7). Group I served as control. Rats in group II - V were exposed to $AlCl_3$ (100 mg/kg) to induce AD. Group III - V rats were treated with 5 mg/kg donepezil, 5 and 10 mg/kg HS-AuNPs, respectively, for 14 days. Behavioral tests were carried out on the rats on day 28 and 42. At the end of animal experiment, rats were sacrificed and used for various biochemical assays and gene expression. The AD rats showed memory and learning impairment, and these conditions were ameliorated by HS-AuNPs. Significant ($p < 0.05$) elevation in the activities of acetylcholinesterase, monoamine oxidase and adenosine deaminase, as well as malondialdehyde levels was noted. A significant reduction in the activities of superoxide dismutase (SOD), glutathione peroxidase (GPx) and reduced glutathione (GSH)

* Corresponding author.
E-mail address: anadozieso@abuad.edu.ng (S.O. Anadozie).
Peer review under responsibility of King Saud University.

Production and hosting by Elsevier

https://doi.org/10.1016/j.arabjc.2023.104604

noted in $AlCl_3$-induced rats were ameliorated by the 5 and 10 mg/kg b.w. doses of HS-AuNPs. In addition, the increased mRNA expression of cyclooxygenase-2 (COX-2) and beta-secretase 1 (BACE-1) caused by $AlCl_3$ were assuaged by the HS-AuNPs treatment. Based on the activities of HS-AuNPs against $AlCl_3$-induced AD, HS-AuNPs could be considered a potential therapeutic agent for managing AD.

1. Introduction

Alzheimer's disease (AD) is a neurodegenerative disease characterized by the deterioration of the nerve cells and neural connections in the brain's cerebral cortex. Individuals with this disease, usually the older adults are seen with abnormalities in the brain tissues and impairment of cognitive functions (DeTure and Dickson 2019). Pathological features of AD include the formation of amyloid beta (Aβ) plaques and neurofibrillary tangles (DeTure and Dickson 2019). Accumulation of Aβ plaques lead to neurodegeneration which interferes with the synaptic communication between neuron-to-neuron. Tau tangles, on the other hand, block the transport of nutrients and other essential molecules within the neurons (Mietelska-Porowska et al., 2014). Although the pathogenesis of AD is not fully known, Aβ aggregates has been associated with oxidative stress (OS) (Cheignon et al., 2018).

Aluminum is a metallic element primarily found in the air, food, drinking water, pharmaceutical and agrochemical products. Over time, its accumulation in the human body either naturally or occupationally, can lead to organ toxicity (Igbokwe et al., 2019). Aluminum chloride ($AlCl_3$) can cross the blood–brain barrier (BBB), altering the axonal transports and synaptic clefts, thus, making the brain a major target organ for aluminum toxicity (Liaquat et al., 2019). Exposure of experimental animals to $AlCl_3$ could result in behavioral and cognitive deficits, cholinergic neuronal loss, amyloid plaques and neurofibrillary tangles formation, which are pathological features of AD (ELBini-Dhouib et al., 2021). Therefore, $AlCl_3$ was used in the present study to mimic sporadic AD-like disorder.

Alzheimer's disease poses a great threat to human health and remains incurable till date. Because of the nature of the brain, which is surround by BBB, drug delivery to affected areas in the brain remain difficult and therefore, limits the effective treatment of AD (Dong 2018). The use of drugs such as acetylcholinesterase inhibitors and *N*-methyl-D-aspartate receptor antagonists have been reported to be less effective. This is because they do not explicitly cure or slow the progression of the disease but only moderately improve cognitive functions and manage the associated symptoms (Breijyeh and Karaman 2020). In addition, these drugs lack tissue-specificity, resulting in adverse effects such as cardiovascular and genitourinary diseases (Ruangritchankul et al., 2021). Therefore, it is necessary to use treatment approach with fewer side effects in managing AD. Medicinal plant-based products are a better option because of their biological activities, availability, fewer side effects, and cost-effectiveness (Roy 2018).

Hibiscus sabdariffa (*H. sabdariffa* (HS)) commonly called "Roselle" belongs to the Malvaceae family of plant. It is widely grown in tropical and subtropical regions of West Africa, India and Egypt (Riaz and Chopra 2018). The dry red calyces of the plant are used in the preparation of hibiscus tea locally called "zobo" in Nigeria and sorel tea in some parts of Asia. The plant is traditionally used for managing hypertension, diabetes, and obesity (Jalalyazdi et al., 2019, Yusni and Meutia 2020). Its ethnopharmacological properties include anti-inflammatory, anti-cancer, antimicrobial and antioxidant activities (Riaz and Chopra 2018, Izquierdo-Vega et al., 2020). Most medicinal plants lack systemic stability and availability hence, their therapeutic potency is greatly limited (Conte et al., 2016).

Metallic nanoparticles (NPs) have wide range of application in food and cosmetics industries, biomedical and pharmaceuticals (Khan et al., 2019). Gold nanoparticles (AuNPs) among other metallic NPs are efficient in biomedical field because of their size, stability, biocompatibility, large surface area and optical properties (Patra et al., 2018). Unlike the chemical and physical methods of NPs synthesis, a biological approach is ecofriendly, safe, and can be scaled up for larger NPs production (Anadozie et al., 2021). In addition, the plant-based biological synthesis possesses phytochemicals that serve therapeutic purposes and therefore was employed in the present study. Nanoparticles synthesized from *H. sabdariffa* have been reportedly used in several studies for the management of cancer (Zangeneh and Zangeneh 2020) and diabetes (Bala et al., 2015); however, none has been reported for AD. To the best of our knowledge, our study will be the first to report the synthesis of AuNPs using aqueous extract of *H. sabdariffa* calyces and its potential in managing AD-like disorder. The present study aimed to investigate the ameliorative potential of *H. sabdariffa* synthesized-AuNPs against $AlCl_3$-induced memory deficits through the inhibition of COX-2/BACE-1 mRNA expression in rats.

2. Materials and methods

2.1. Chemicals and reagents

Tetrachloroauric acid was procured from Sigma Chemical Co. (St. Louis, MO, USA). Aluminum chloride was procured from Alfa Aersa Belgore, (Germany). Donepezil hydrochloride (Dnpz) was procured from Milpharm labs limited, (United Kingdom). Gene specific primers (cyclooxygense-2 (COX-2), beta-secretase 1 or beta-site amyloid precursor protein cleaving enzyme 1 (BACE-1) and brain-derived neurotrophic factor (BDNF)) for PCR were purchased from Inqaba Biotech, South Africa.

2.2. Plant authentication and extraction

The *H. sabdariffa* calyces were obtained from a personal garden in Ado Ekiti, Ekiti State, Nigeria. The plant was identified and authenticated at the Forestry Research Institute of Nigeria (FRIN) Ibadan, Nigeria with a reference number 112433. The air-dried HS calyces were blended into fine particles. To a beaker containing 100 mL of distilled water, 10 g of the powder plant material was added, and boiled in a water bath at 80 °C to obtain crude extract, as it is being done traditionally. The crude extract was then filtered and used for the synthesis of AuNPs (Adewale et al., 2020).

2.3. Synthesis and characterization of H. Sabdariffa synthesized gold nanoparticles (HS-AuNPs)

The AuNPs was successfully synthesized using crude extract of *H. sabdariffa* according to the method described by Anadozie

et al., (2022) with slight modification. Briefly, 10 mg/mL of the plant extract was added to 1 mM gold (Au) solution (optimized concentrations). The mixture was continuously stirred at a temperature of 100 °C until a purple color was observed within 10 min. The NPs solution was stirred for additional 20 min without heat, and the formed HS-AuNPs washed twice at a centrifugal speed of 10,000 *g* for 15 min at 4 °C to remove the uncapped phytochemicals. The AuNPs solution was lyophilized to powder form. The surface plasmon resonance (SPR) of the HS-AuNPs was measured by ultraviolet–visible (UV–vis) spectrophotometer in the range of 350–750 nm. Further characterization of the HS-AuNPs was performed for particle size distribution, stability, surface charge, morphology, crystallinity, and functional groups present on the surface of the AuNPs using dynamic light scattering (DLS), high-resolution transmission electron microscopy (HRTEM) and Fourier transform-infrared spectroscopy (FT-IR).

2.4. Experimental animals and design

Forty-two (42) male Wistar rats, weighing between 120 and 150 g were used in the present study. The animals were procured from the animal house, Department of Veterinary Medicine, University of Ibadan, Oyo State, Nigeria. The animals were kept in polypropylene cages and maintained at room temperature (25 ± 2 °C) and relative humidity (55 ± 10 %) with access to a 12-h light/dark cycle. The rats were fed with commercially available rat chow and water *ad libitum*. The animal experiment was performed following the International and National guidelines for the use of experimental animals.

2.5. Experimental design

After the acclimatization period, animals were randomly divided into six groups comprising of seven animals each. Group I served as control. Rats in group II served as AD control and were orally given 100 mg/kg b.w. $AlCl_3$. Group III rats served as positive control and orally received 100 mg/kg b.w. $AlCl_3$ and treated with 5 mg/kg b.w. Dnpz. Group IV and V orally received 100 mg/kg b.w. $AlCl_3$ and treated with 5 and 10 mg/kg b.w. HS-AuNPs, respectively. Group VI rats orally received 10 mg/kg b.w. HS-AuNPs only. The animal experiment lasted for 42 days where rats in group II – V were exposed to $AlCl_3$. At day 28 and 42 behavioral studies were performed to confirm the induction of AD following the methods described by Shunan et al., (2021) and Bazzari et al., (2019). The predisposition of the experimental rats to $AlCl_3$ (day 1 to 28) exposed the animals to an early signs of sporadic AD. Co-treatment of $AlCl_3$ with Dnpz or HS-AuNPs was done from day 28 to day 42 (Fig. 1). The HS-AuNPs (5 and 10 mg/kg) doses were selected following the preliminary toxicological evaluation performed in our laboratory (data not shown). Treatments (Dnpz and HS-AuNPs were administered to the rats 1 h after $AlCl_3$ intoxication.

2.6. Behavioral test

Behavioral assessment was carried out on the test animals on day 28 and 42 to confirm if $AlCl_3$ initiated memory deficit (one of the symptoms of AD) using the novel object recognition (NOR), Y-maze and elevated plus maze (EPM) tests. The NOR test was performed according to the method described by Antunes and Biala (2012) to assess the learning and recognition memory in $AlCl_3$-induced AD rats. The Y-maze test was performed to examine the functional and cognitive memory of the AD rats following the method of Anadozie et al., (2019). The EPM test was performed following the method of Pellow et al., (1985) to examine test animals' anxiety levels, memory, and spatial learning. A video tracking device was setup to monitor entries made by each rat in the different neurobehavioral analyses studied. The apparatus was wiped with 70 % ethanol after each test. Time spent by the rats exploring the familiar and novel objects, as well as the discrimination and recognition index were calculated in the NOR test. The number of arm entries and animals' predisposition toward navigating a less recently visited arm was examined in Y-maze. In EPM, the number of entries into open arms, % open arm entries and % total time spent in open arms were analyzed.

2.7. Preparation of brain tissue homogenate

Twenty-four (24) h after HS-AuNPs treatments, the fasted rats were sacrificed via anesthesia (isoflurane inhalation). The brains were rapidly isolated, mopped of blood stains, and weighed. A little portion of the hippocampus was cut out for mRNA gene expression. The remaining part of the hippocampus and cerebral cortex of the brain were rinsed in cold phosphate buffer (0.1 M, pH 7.4) and subsequently homogenized in four volumes of the phosphate buffer. The tissue homogenate was centrifuged at 10,000 *g* for 10 min at 4 °C to obtain a clear supernatant for biochemical analyses.

2.8. Measurement of neurological and oxidative biomarkers in the tissue homogenate

Acetylcholinesterase (AChE) and monoamine oxidase (MAO) activities were estimated according to the methods described by Ellman et al., (1961) and Green and Haughton (1961). Adenosine deaminase activity (ADA) was assessed using the method described by Giusti (1974). Lipid peroxidation was

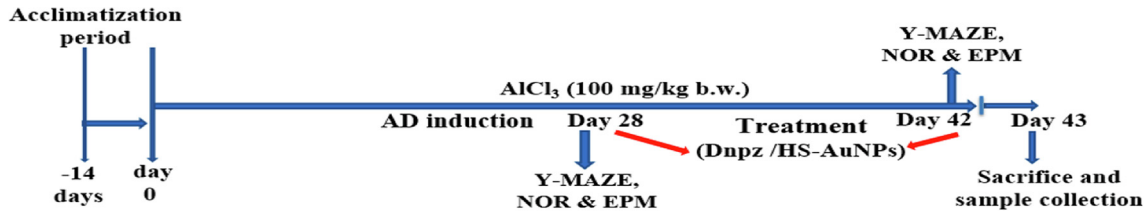

Fig. 1 Illustration of the experimental design timeline. $AlCl_3$ - aluminum chloride; AD - Alzheimer's disease; Dnpz - donepezil; HS-AuNPs - *Hibiscus sabdariffa*-synthesized gold nanoparticles, NOR - novel object recognition, EPM - elevated plus maze.

performed to determine the level of malondialdehyde (MDA) adducts in the tissue homogenate as described by Ohkawa et al., (1979). Antioxidant activities such as superoxide dismutase (SOD), glutathione peroxidase (GPx) and reduced glutathione (GSH) were evaluated in the tissue homogenate by the methods of Alía et al., (2003), Wendel (1981) and Ellman (1959) respectively.

2.9. Quantitative reverse transcription-polymerase chain reactions (RT-RCR) analysis

2.9.1. Isolation of total RNA

Isolation of total RNA from the hippocampus brain region of the rats was performed using Trizol reagent (Gibco). The RNA quantity (concentration (μg/ml) = 40 × A_{260}) and quality (≥1.8) were measured spectrophotometrically using the ratio A_{260}/A_{280} (A = absorbance).

2.9.2. Conversion of cDNA

The conversion of DNA-free RNA to cDNA was performed by incubating 40 μg of the total RNA at 37 °C for 1 h using M−MuLV Reverse Transcriptase Kit (NEB) as instructed on the leaflet by the manufacturer. The Snap gene software was used in the present study for primers design.

2.9.3. Polymerase chain reaction amplification

Amplicons were resolved on 1.5 % agarose gel in Tris (RGT reagent)-Borate-EDTA buffer (pH 8.4) and ethidium bromide staining was used for visualization. Quantification of the amplicon bands was done using Image-J software. The following primers of interest were used in this study:

Target	Forward '5–3	Reverse '5-3′	Base pair
genes			
COX-2	TCAGCCATGCA GCAAATCC	GATTCTTGTCAGA AACTCAGGCG	70
BACE-1	CCCCCACAGAC GCTCAACAT	GGTGTAGGGCACA TACACAGAC	56
BDNF	TTCCCTCAG CTCGCCAC	TCTCACCTGGTGGA ACTCAG	28
B-Actin	CCACCAGTTCG CCATGGAT	CCCACCATCACA CCCTGG	42

2.10. Data analysis

Data analysis was performed where applicable using one-way analysis of variance (ANOVA) on GraphPad Prism 8.01, 2018 (GraphPad software, Inc, San Diego, USA), followed by Tukey's post hoc test. Results were represented as mean ± standard deviation (SD), n = 7 of triplicate readings. Statistical significance at $p < 0.05$ was considered in all cases.

3. Results

3.1. Preliminary phytochemical screening of *H. sabdariffa* calyx

The qualitative screening of bioactive metabolites in the crude extract of *H. sabdariffa* calyces are revealed in Table 1.

Table 1 Qualitative screening of phytochemicals from *H. sabdariffa*.

Phytochemicals	Observation
Alkaloids	+
Flavonoids	+
Glycosides	+
Phenols	+
Saponins	+
Tannins	+
Terpenoids	+

+ signifies the presence of bioactive metabolite.

3.2. Gold NPs synthesis

The formation of HS-AuNPs was visually observed for a change in color of the reaction mixture from wine red to purple within 10 min of adding the HS extract to the Au solution.

3.3. Gold NPs characterization

3.3.1. Stability testing of H. sabdariffa synthesized-AuNPs

The SPR and stability testing of the HS-AuNPs was spectrophotometrically measured using UV–vis absorption spectroscopy. The HS-AuNPs maintained a stable absorption maximum (λ^{max}) of 534 nm from the first 1 h to 48 h (Fig. 2, supplementary 1). In addition, no sign of agglomeration was observed in the synthesized HS-AuNPs.

3.3.2. Hydrodynamic size distribution, morphology, and crystallinity of H. sabdariffa synthesized-AuNPs

The DLS measurement revealed an average hydrodynamic diameter of 23.82 ± 0.22 nm and polydispersity index (PDI) of 0.378 ± 0.02 nm for the synthesized HS-AuNPs in liquid medium. In addition, the zeta potential measurement of the HS-AuNPs showed a surface charge of −19.1 ± 0.96 mV. The HRTEM microscopic image revealed mostly spherical-shaped AuNP cores (Fig. 3 A – B). As analyzed by image J, an average size of 12.99 ± 4.04 nm was obtained for the synthesized AuNPs (Fig. 3 C). The SAED image showed the crystalline nature of the HS-AuNPs with a ring pattern

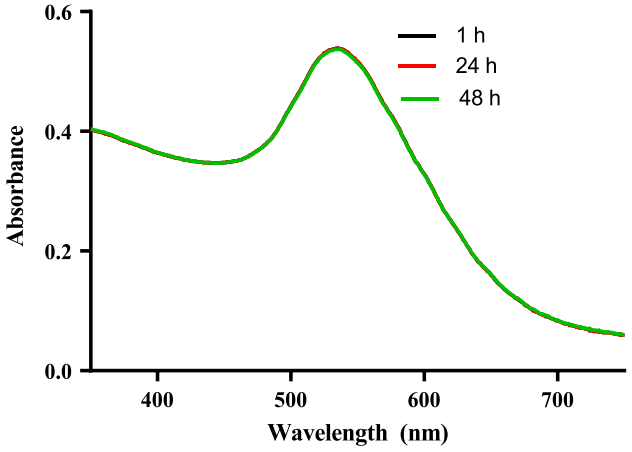

Fig. 2 UV–vis absorption spectrum of *H. sabdariffa* synthesized-AuNPs showing SPR band at different time interval.

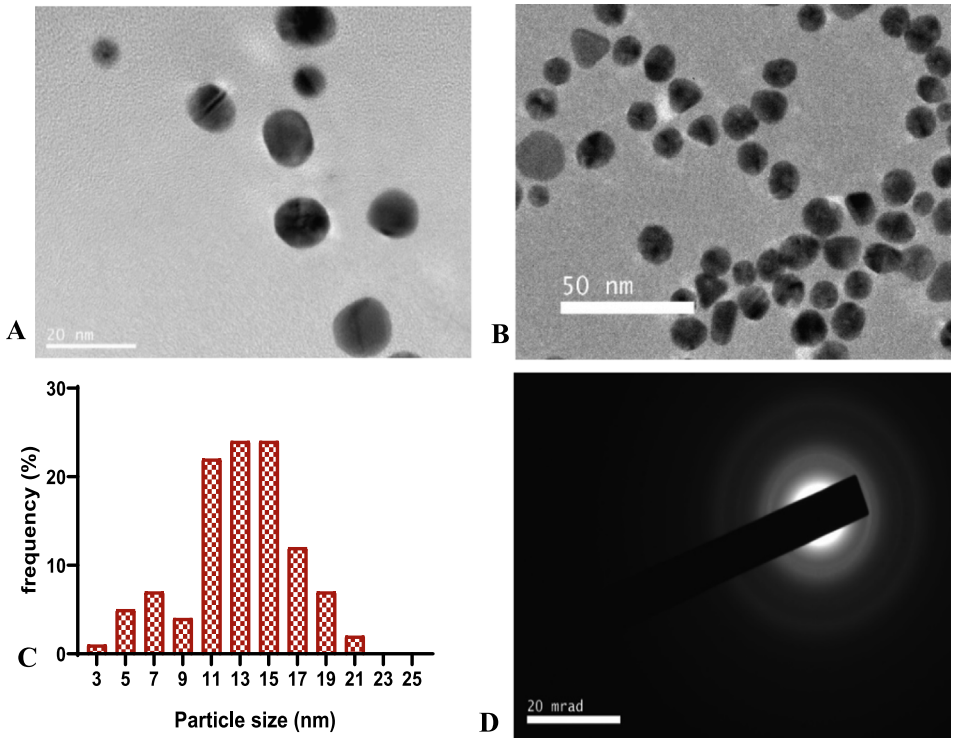

Fig. 3 HRTEM micrographs and histogram images of *H. sabdariffa* synthesized-AuNPs at 20 nm scale bar (A), 50 nm scale bar (B), histogram of particle size distribution (C), SAED image (D).

corresponding to the Bragg's reflections ring (111), (200), (220), and (311) of face centered cubic (fcc) structure of metallic Au, JCPDS no. 04–0784 (Fig. 3 D).

3.3.3. Functional groups present on the surface of H. sabdariffa plant extract and its synthesized-AuNPs

Table 2 depicts the FTIR absorption values and functional groups present on the surface of HS extract and its synthesized-AuNPs. Two characteristics peaks different from other absorption peaks were observed in both the plant extract and its synthesized-AuNPs (Table 2, supplementary 2). These include the intense peaks at 1633.93 and 1632.70 cm^{-1} and broad peaks at 3333.13 and 3252.65 cm^{-1}, respectively.

3.4. Assessment of behavioral, cognitive, and hippocampal functions of $AlCl_3$-induced AD rats

3.4.1. Novel object recognition (NOR) behavioral test

Fig. 4 shows the effect of HS-AuNPs in enhancing the hippocampal function and recognition memory in $AlCl_3$-induced AD rats using the NOR test. The rats in $AlCl_3$ group performed poorly on day 28 and 42 by significantly ($p < 0.05$) decreasing the time spent in both familiar and novel object when compared to the control (Fig. 4 (A-B)). The treatments (Dnpz and HS-AuNPs) on day 42 restored the impaired cognitive functions. Similarly, in the novel object preference (% (Fig. 4 C)), the ability of rats in the $AlCl_3$ (AD rats) group to recognize the novel object on days 28 and 42 was significantly ($p < 0.05$) reduced when compared to the control group. Treatment of the AD rats with HS-AuNPs at 10 mg/kg b.w. significantly ($p < 0.05$) increased the novel object preference on day 42 when compared to the control, $AlCl_3$, and Dnpz groups, respectively.

Aluminum-exposed rats performed very poorly in the discrimination index analysis on days 28 and 42 as shown in Fig. 4 D. Statistically, in comparison with the control, the AD rats could not distinguish between familiar and novel objects. Treatment with tested doses of Dnpz and HS-AuNPs on day 42 significantly ($p < 0.05$) increased the familiar and novel object when compared with the $AlCl_3$ group. The

Table 2 Fourier transform infrared absorption spectroscopic measurement of *H. sabdariffa* synthesized gold nanoparticles.

HS extract wavelength (cm^{-1})	HS-AuNPs wavelength (cm^{-1})	Bonds	Functional groups
3333.13	3252.65	O—H stretch N—H stretch	Alcohols, phenols Aliphatic secondary Amines
2106.83	2036.72	C≡C stretching	Alkyne
1633.93	1632.70	C=C stretch	Alkene
–	1416.40	O—H bending	Alcohol
1157.26	1082.71	C—O stretch	Aromatic alcohols
1022.68	979.46	=C—O—C stretch	Ethers

HS - *Hibiscus sabdariffa*, HS-AuNPs - *Hibiscus sabdariffa* synthesized gold nanoparticles.

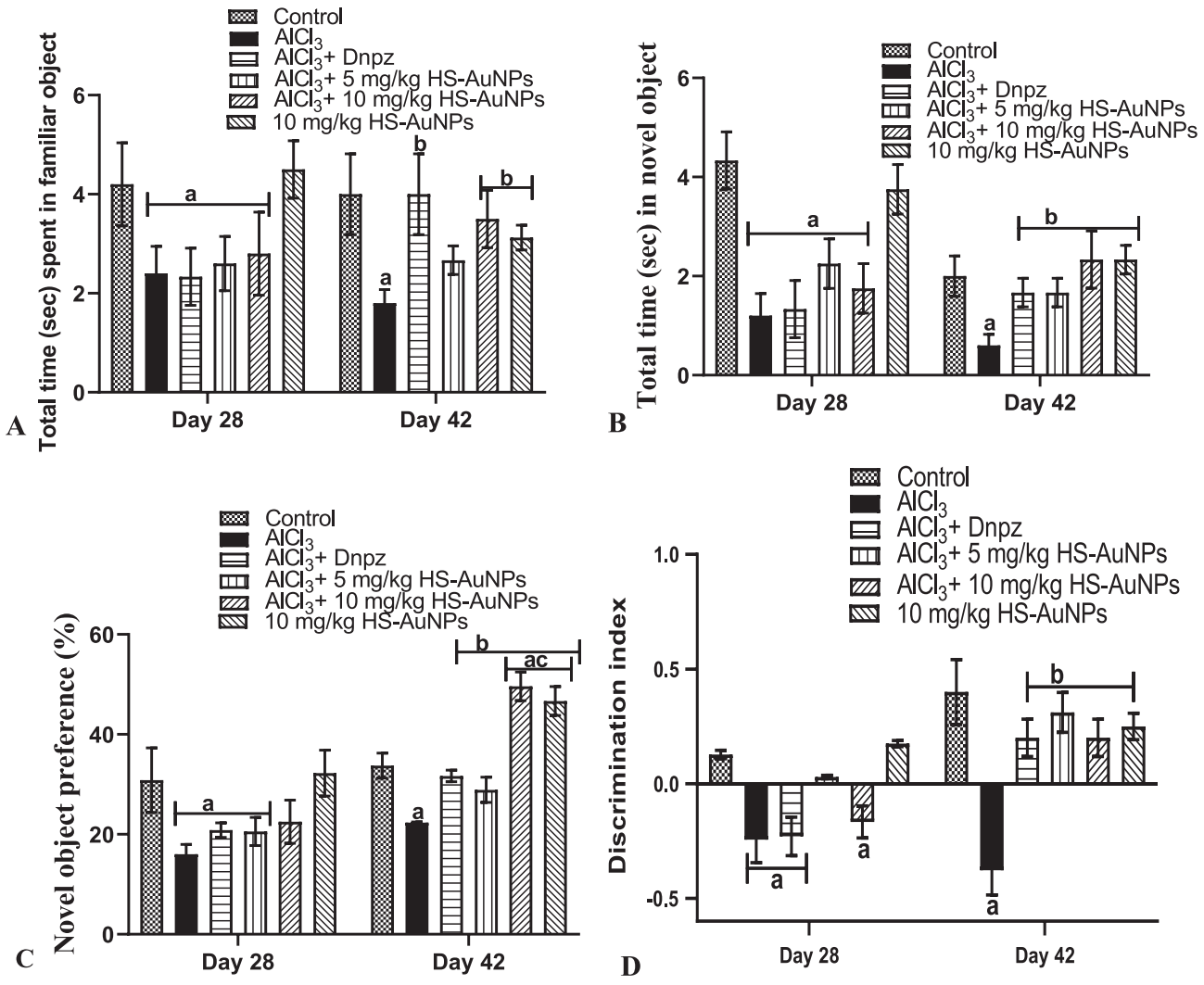

Fig. 4 Effect of *H. sabdariffa* synthesized-AuNPs on the cognitive function test of $AlCl_3$-induced AD rats. Familiar object (A), novel object (B), % novel object preference (C), discrimination index (D). Results are expressed as mean ± SD (n = 7). $^{a}p < 0.05$ vs control, $^{b}p < 0.05$ vs $AlCl_3$ group, $^{c}p < 0.05$ vs Dnpz group.Legend: $AlCl_3$ - aluminum chloride; Dnpz – donepezil; HS-AuNPs- *Hibiscus sabdariffa* synthesized-gold nanoparticles.

treatment doses of HS-AuNPs exhibited similar result as that of Dnpz group.

3.4.2. Y-maze behavioral test (memory index)

Table 3 shows a significant ($p < 0.05$) reduction in the % spontaneous alternation in the $AlCl_3$-induced rats on days 28 and 42 when compared to the control. A similar result was noted in Dnpz and 5 mg/kg b.w. HS-AuNPs treated groups on day 42. The spatial working memory of the AD rats were however, restored by HS-AuNPs treated groups at 10 mg/kg b.w. on day 42 by a significant ($p < 0.05$) increase in the % spontaneous alternation of rats when compared with the $AlCl_3$ and Dnpz groups, respectively.

In addition, comparing the $AlCl_3$-exposed rats and the treated groups to the control on days 28 and 42, no significant ($p > 0.05$) difference was observed in the number of arm entries (locomotor activity), except for the rats treated with 10 mg/kg b.w. HS-AuNPs only where a significant ($p < 0.05$) increase was observed in the number of arm entries on day 42 when compared with the Dnpz group.

3.4.3. Elevated plus maze (EPM) behavioral test

In the EPM test, a significant ($p < 0.05$) decrease in the total arm entries was observed in groups exposed to $AlCl_3$ on day 28 when compared with the control group. However, on day 42 no significant ($p > 0.05$) difference was observed in the $AlCl_3$ group when compared to the control, Dnpz and HS-AuNPs treated groups, respectively. Although not significant, an increase in the total arm entries was observed in the 10 mg/kg b.w. HS-AuNPs when compared to $AlCl_3$ (Fig. 5 A).

Similarly, a significant ($p < 0.05$) decrease in the % open arm entries was observed in the $AlCl_3$ group and Dnpz treated group on days 28 and 42 when compared with the control. Treatment with HS-AuNPs at 10 mg/kg b.w., restored the anxiolytic memory impairment caused by $AlCl_3$ administration with a marked significant ($p < 0.05$) increase in the % open

Table 3 Effect of HS-AuNPs on the spatial working memory of $AlCl_3$-induced AD rats using Y-maze.

Groups	Spontaneous alternation (%)		Number of arm entries	
	28 days	42 days	28 days	42 days
Control	93.3 ± 10.00	90.0 ± 11.54	5.25 ± 1.50	5.25 ± 1.50
$AlCl_3$	49. 0 ± 7.41[a]	54.6 ± 6.33[a]	5.60 ± 1.34	5.25 ± 1.26
$AlCl_3$ + Dnpz	39.2 ± 3.29[a]	47.5 ± 6.45[a]	4.00 ± 2.00	3.75 ± 0.96
AlCl3 + 5 mg/kg HS-AuNPs	39.5 ± 4.78[a]	50.0 ± 8.16[a]	4.67 ± 0.57	4.25 ± 0.96
$AlCl_3$ + 10 mg/kg HS-AuNPs	53.2 ± 9.58[a]	77.5 ± 6.45[bc]	5.66 ± 0.50	5.50 ± 1.29
10 mg/kg HS-AuNPs	88.3 ± 9.13[bc]	85.0 ± 12.91[bc]	6.75 ± 1.52[c]	6.50 ± 1.29[c]

Results are expressed as mean ± SD (n = 7). ap < 0.05 vs control, bp < 0.05 vs AlCl3 group, cp < 0.05 vs Dnpz group.
Legend: AlCl3 - aluminum chloride; Dnpz – donepezil; HS-AuNPs- Hibiscus sabdariffa synthesized-gold nanoparticles.

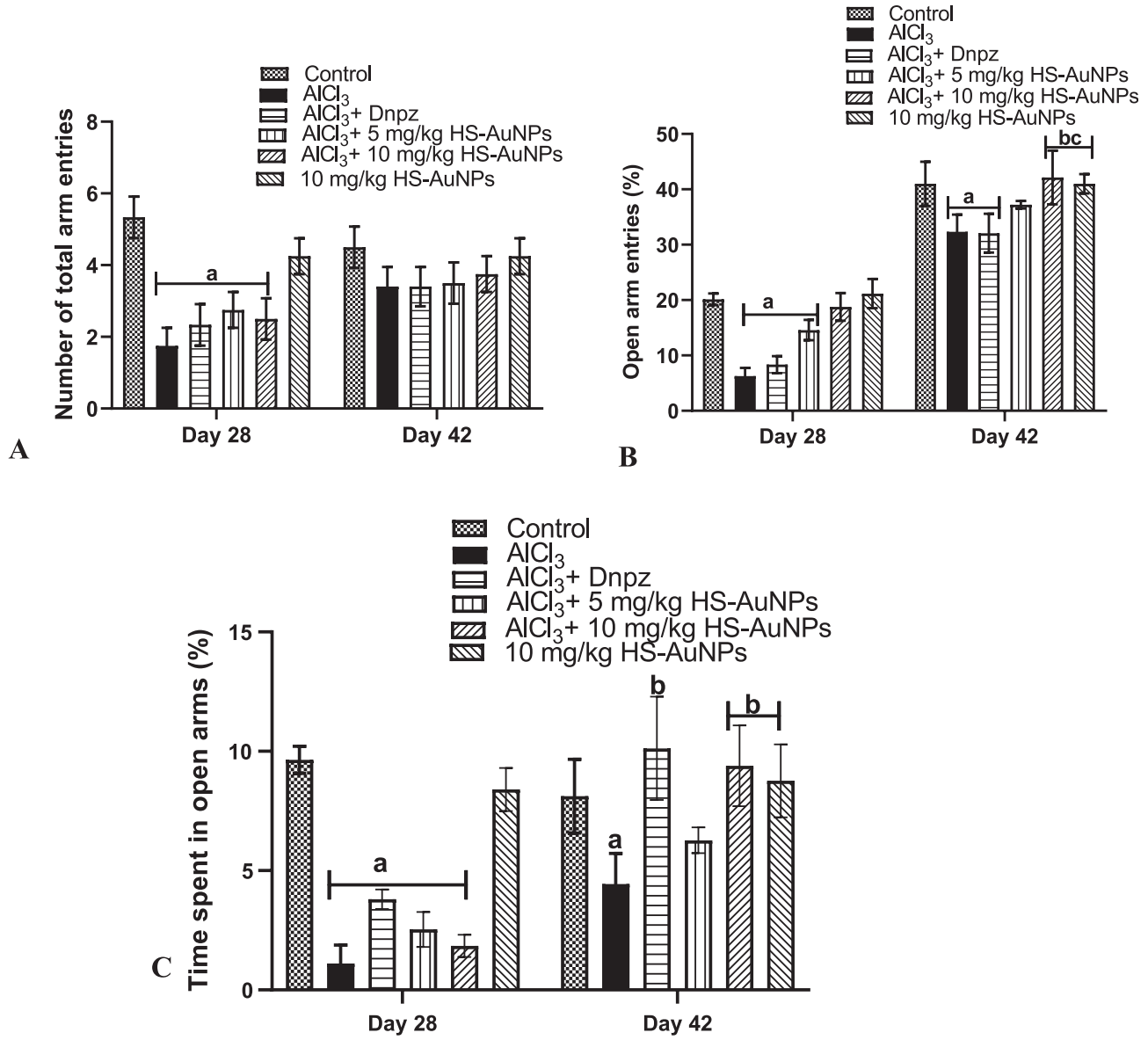

Fig. 5 Effect of *H. sabdariffa* synthesized-AuNPs on the cognitive function test of $AlCl_3$-induced AD rats. Number of total arm entries (A), % open arm entries (B), % time spent on open arms (C) in elevated plus maze test. Results are expressed as mean ± SD (n = 7). [a]p < 0.05 vs control, [b]p < 0.05 vs $AlCl_3$ group, [c]p < 0.05 vs Dnpz group. Legend: $AlCl_3$ - aluminum chloride; Dnpz – donepezil; HS-AuNPs- *Hibiscus sabdariffa* synthesized-gold nanoparticles.

arm entries on day 42 when compared with the $AlCl_3$ and Dnpz groups, respectively (Fig. 5 B). Also, the administration of $AlCl_3$ in rats caused a significant ($p < 0.05$) reduction in the total time spent in the open arm (%) at days 28 and 42 when compared with the control (Fig. 5 C). A significant ($p < 0.05$) increase in the total time spent in open arm (%) was observed in Dnpz and 10 mg/kg b.w. HS-AuNPs at day 42 when compared with the $AlCl_3$ group.

3.5. Relative organ weight of rats $AlCl_3$-induced AD rats

Oral administration of $AlCl_3$ to rats caused a significant ($p < 0.05$) reduction in the body weight gain of rats when compared with the control. In comparing the various doses of Dnpz and HS-AuNPs to the $AlCl_3$ group, a significant increase was observed (Fig. 6 A).

In addition, a significant increase in the relative brain weight of rats was observed in the $AlCl_3$ and Dnpz groups when compared with the control (Fig. 6 B). The HS-AuNPs treatment at tested doses were able to ameliorate the effect of $AlCl_3$ on the rat's brain.

3.6. Biochemical assays

3.6.1. Neuronal acetylcholine inhibitors and neuromodulator indices

The effect of HS-AuNPs on AChE, MAO and ADA activities in $AlCl_3$-intoxicated rats are shown in Fig. 7 (A - C). Oral administration of $AlCl_3$ significantly ($p < 0.05$) elevated the AChE and MOA activities in AD rats compared with the control (Fig. 7 A and B). Treatment with Dnpz and HS-AuNPs at tested doses were able to attenuate the effect of $AlCl_3$ in the AD rats by significantly ($p < 0.05$) decreasing the acetylcholine inhibitors activities when compared with the $AlCl_3$ group. A significant ($p < 0.05$) decrease in the MAO activity was also observed in the AD rats treated with HS-AuNPs at a dose of 10 mg/kg b.w. when compared with the Dnpz group (Fig. 7 B).

As revealed in Fig. 7 C, a significant ($p < 0.05$) increase in the activity of ADA was observed in the $AlCl_3$ group when compared with the control. Treatment with Dnpz and HS-AuNPs at tested doses significantly ($p < 0.05$) decreased the activity of ADA when compared with the $AlCl_3$ group.

3.7. Oxidative and antioxidant biomarkers

As displayed in Table 4, oral administration of $AlCl_3$ significantly ($p < 0.05$) increased the MDA levels in AD rats when compared with the control. Treatment with Dnpz and HS-AuNPs significantly ($p < 0.05$) reduced the MDA levels when compared to the $AlCl_3$ group.

Furthermore, the administration of $AlCl_3$ significantly ($p < 0.05$) reduced the neuronal SOD and GPx activities in the $AlCl_3$ (AD) group when compared with the control. In the GPx activities, Dnpz and 5 mg/kg b.w. HS-AuNPs treated groups showed similar results as the $AlCl_3$ group when compared with the control. Treatment with HS-AuNPs at tested doses mitigate the radical effect of $AlCl_3$ in the rats by a significant ($p < 0.05$) increase in the SOD and GPx activities (Table 3).

In addition, a significant ($p < 0.05$) decrease in the neuronal GSH activity was observed in the $AlCl_3$ group when compared with the control. The 5 mg/kg b.w. HS-AuNPs treated group exhibited similar result as the $AlCl_3$ group. The HS-

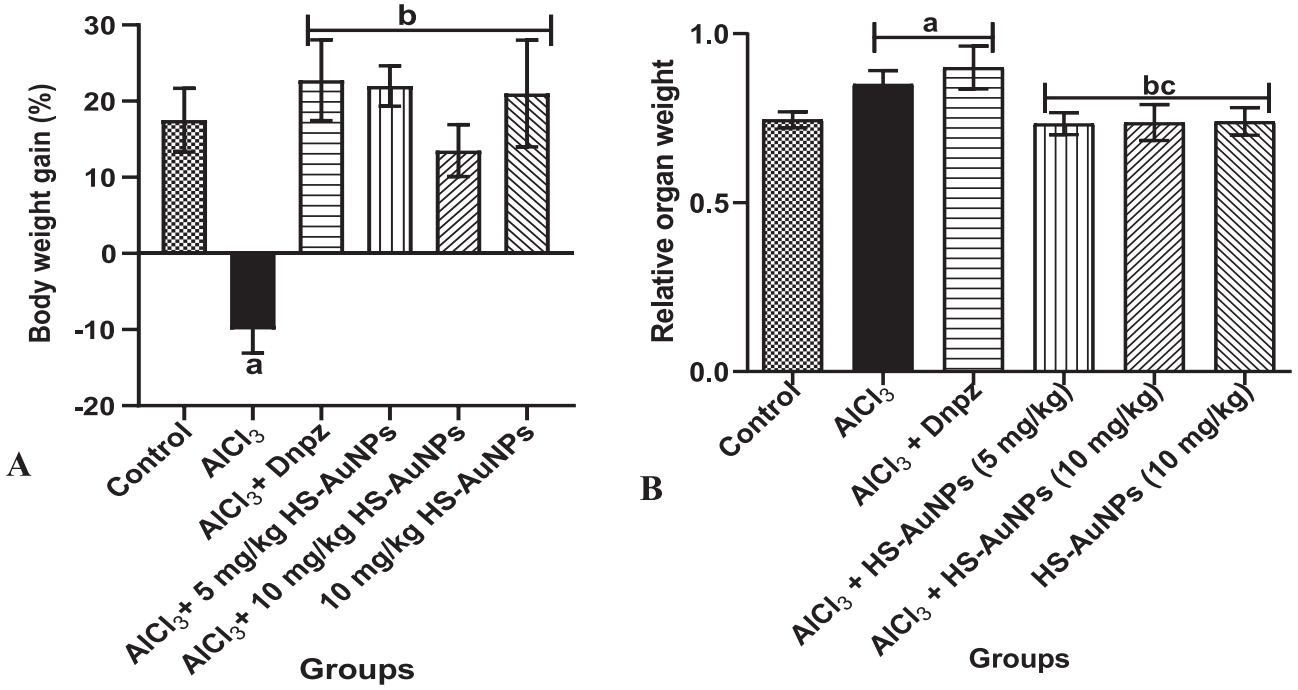

Fig. 6 Effect of *H. sabdariffa* synthesized-AuNPs on the body weight gain (A) and relative brain weight (B) of $AlCl_3$-induced AD rats. Results are expressed as mean ± SD (n = 7). [a]$p < 0.05$ vs control, [b]$p < 0.05$ vs $AlCl_3$ group, [c]$p < 0.05$ vs Dnpz group. Legend: $AlCl_3$ - aluminum chloride; Dnpz – donepezil; HS-AuNPs- *Hibiscus sabdariffa* synthesized-gold nanoparticles.

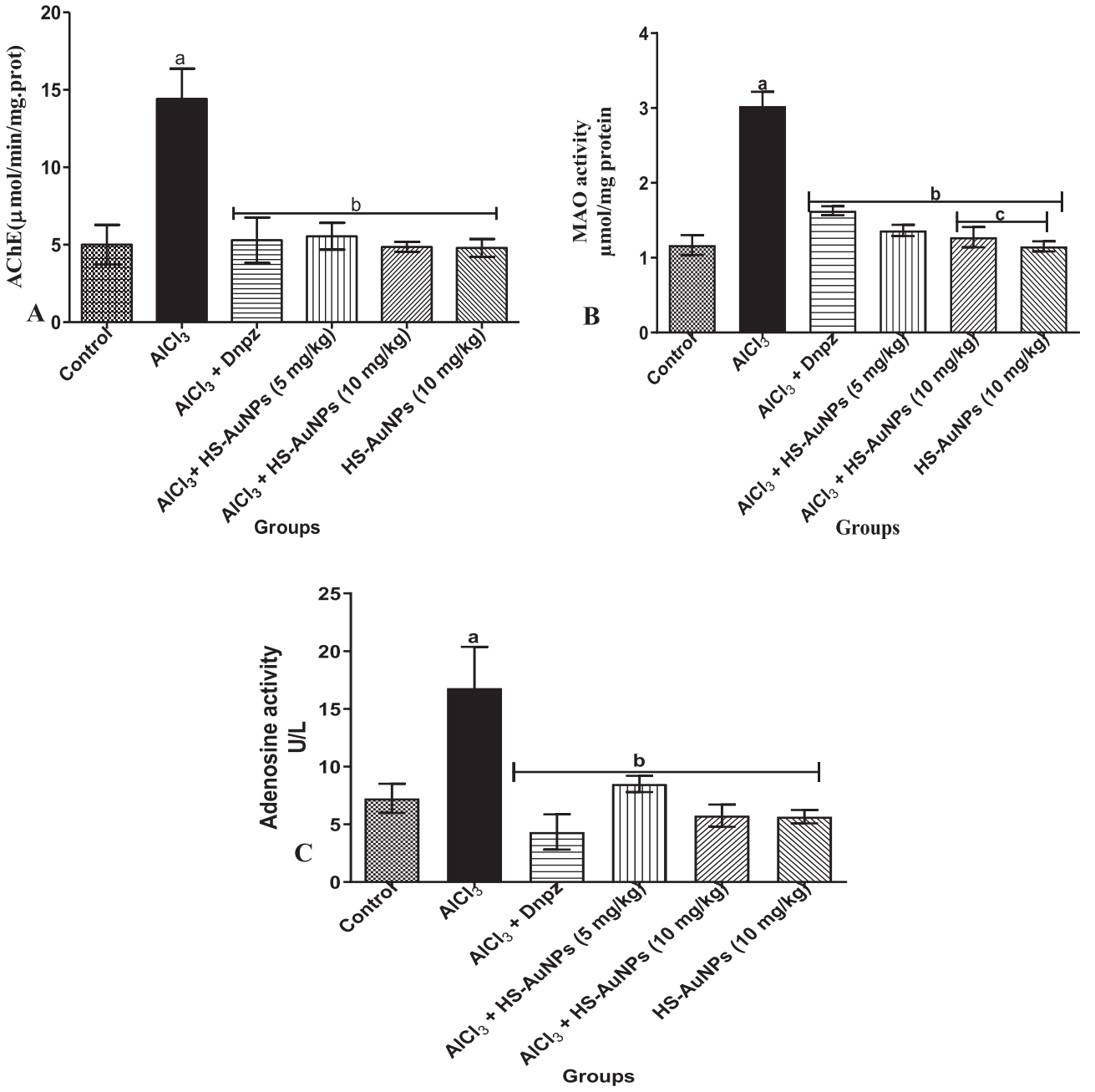

Fig. 7 Effect of *H. sabdariffa* synthesized-AuNPs on acetylcholinesterase (A), monoamine oxidase (B), adenosine deaminase (C) activities in the brain of $AlCl_3$-induced AD rats. Results are expressed as mean ± SD (n = 7). $^{a}p < 0.05$ vs control, $^{b}p < 0.05$ vs $AlCl_3$ group, $^{c}p < 0.05$ vs Dnpz group. Legend: $AlCl_3$ - aluminum chloride; Dnpz – donepezil; HS-AuNPs- *Hibiscus sabdariffa* synthesized-gold nanoparticles.

AuNPs treatment at both doses significantly ameliorated the reduced GSH activity instigated by $AlCl_3$ administration.

3.8. mRNA expression

The polymerase chain reaction analyses of COX-2, BACE-1 and BDNF mRNA expression in the hippocampus of AD rats were evaluated as shown in Fig. 8 A-D.

Oral administration of $AlCl_3$ significantly ($p < 0.05$) increase mRNA expression of COX-2 and BACE-1 in the hippocampus of AD rats ($AlCl_3$ group) and 5 mg/kg b.w., HS-AuNPs treated group when compared with the control (Fig. 8 A – B and D). The AD rats treated with Dnpz and HS-AuNPs at tested doses significantly ($p < 0.05$) decreased mRNA expressions of COX-2 and BACE-1 when compared with $AlCl_3$ group (Fig. 8 A – B, and D). A significant ($p < 0.05$) increase in the BACE-1 mRNA expression was observed in the 5 mg/kg b.w HS-AuNPs when compared with the $AlCl_3$ group (Fig. 8 B). Statistically, a significant ($p < 0.05$) increase in the mRNA expression of COX-2 and

Table 4 Effect of crude extract of *H. sabdariffa* synthesized- AuNPs on $AlCl_3$–induced Alzheimer disease in rats as indicated by neural oxidative and antioxidant biomarkers.

Treatment group	MDA (nm/ mg prot)	SOD (U/mg prot)	GPx(U/mg prot)	GSH(U/mg prot)
Control	0.4 ± 0.03	110.7 ± 3.83	115.4 ± 8.29	67.0 ± 3.48
$AlCl_3$ alone	0.9 ± 0.09^{a}	68.8 ± 6.32 ^{a}	63.2 ± 2.92^{a}	44.5 ± 1.76^{a}
$AlCl_3$ + Dnpz	0.4 ± 0. 09^{b}	107.9 ± 1.64^{b}	98.1 ± 4.59^{ab}	65.6 ± 3.01^{b}
$AlCl_3$ + 5 mg/kg HS-AuNPs	0.5 ± 0.08^{b}	106.2 ± 6.23^{b}	94.9 ± 6.31^{a}	58.6 ± 2.37^{ab}
$AlCl_3$ + 10 mg/kg HS-AuNPs	0.4 ± 0.03^{b}	104.4 ± 6.11^{b}	107.9 ± 6.11^{b}	61.2 ± 4.70^{b}
10 mg/kg HS-AuNPs	0.4 ± 0.05^{b}	106.6 ± 2.66^{b}	119.0 ± 2.72^{bc}	62.0 ± 1.57^{b}

Results are expressed as mean ± SD (n = 7). ap < 0.05 vs control, bp < 0.05 vs AlCl3 group, cp < 0.05 vs Dnpz group.
Legend: AlCl3 - aluminum chloride; Dnpz – donepezil; GPx - glutathione peroxidase; GSH - reduced glutathione; HS-AuNPs- Hibiscus sabdariffa synthesized-gold nanoparticles; MDA – malondialdehyde; superoxide dismutase (SOD).

BACE-1 were observed in the 5 mg/kg b.w HS-AuNPs when compared with the Dnpz group (Fig. 8 A – B, and D).

A significant ($p < 0.05$) difference was noted in the mRNA expression of BDNF in $AlCl_3$ (AD rats), Dnpz and HS-AuNPs treated groups when compared with the control (Fig. 8 C and D). Increased mRNA expression of BDNF was noted in the Dnpz and HS-AuNPs treated groups when compared with the $AlCl_3$ group. The target mRNA genes were normalized against β-actin as revealed by the band density of the RT-PCR (Fig. 8 D).

4. Discussion

Alzheimer's disease remains the most common cause of dementia, accounting for about 70 % of the 57.4 million cases worldwide. This figure is estimated to be a threefold increase by 2050 (He et al., 2016, Nichols and Vos 2021). Alzheimer's disease is reportedly linked to OS (Zhao and Zhao 2013). Aluminum chloride alters several signaling pathways in the brain, thereby, inducing OS, neuroinflammation and cognitive deficits (Justin-Thenmozhi et al., 2018, ELBini-Dhouib et al., 2021). Therefore, in the present study, we considered $AlCl_3$ a suitable neurotoxicant for inducing AD-like disorder in rats.

The successful synthesis of HS-AuNP could be attributed to the presence of alkaloids, polyphenolics, saponins and glycosides in the crude extract of *H. sabdariffa* calyx. These phytochemicals have been known for their pharmacological properties (Sinha 2019, Rajput et al., 2022), which could be responsible for the ameliorative potential of the HS-AuNPs. In the present study, AuNPs were synthesized using crude extract of *H. sabdariffa* calyces. The phytochemicals in the plant extract serves to reduce the Au^{3+} to Au^{0} and likewise as capping and therapeutic agents (Anadozie et al., 2021). The observed color change in the reaction mixture on adding the plant extract to the Au solution indicates the successful synthesis of HS-AuNPs, which is attributed to the characteristic peak of the SPR (Bawazeer et al., 2021). The SPR absorption maxima of the HS-AuNPs, as revealed by the UV–vis spectroscopy measurement (Fig. 2), suggest that phytochemicals present in the *H. sabdariffa* extract was able to reduce Au^{3+} to Au^{0}.

The hydrodynamic size and PDI value obtained in the present study suggests that the particle in solution was uniformly distributed without agglomeration. These parameters also determine the cellular uptake of the AuNPs (Danaei et al., 2018). The particle size measured on DLS was much larger than the HRTEM measurement. This is because DLS measures NPs in liquid suspension (Mourdikoudis et al., 2018). The size and shape of NPs enhances the delivery of drug across the BBB. Nanoparticles of < 100 nm easily crosses the BBB (Saraiva et al., 2016). The small size and mostly spherical-shaped AuNPs revealed by the HRTEM images of this study could be responsible for the passage of the HS-AuNPs across the BBB. Unlike the peripheral barriers, BBB accommodate only smaller-sized particles because of the tight junctions (zonulae occludentes) in between them (Danaei et al., 2018). Medium-sized AuNPs in the range of 15 nm are the most efficient in crossing the BBB (Ohta et al., 2020). It is worthy of note that the HS-AuNPs produced in our study was within this range.

The polyphenolic compounds present in the plant extract as revealed by the FTIR measurement could be responsible for the reduction of Au^{+} to Au°. The unique peaks shown on the FT-IR chromatogram (supplementary 1) corresponds to the OH, –NH and C═C groups, which denotes the presence of polyphenolic compounds and alkaloids (Singh et al., 2018). Therefore, suggesting their roles in the reduction and stabilization of the HS-AuNPs. Ahmed and Mustafa (2020) reported that a shift in the FT-IR absorption bands could be because of the involvement of plant phytochemicals as reducing agents in the synthesis of NPs. In this study, the slight change in absorption bands of the HS-AuNPs indicates the functional groups responsible for the reduction and formation of the AuNPs.

Memory and learning process are key players in assessing behavioral patterns in AD patients. Therefore, in this study, neurobehavioral assessment was performed on the $AlCl_3$-induced AD rats to assess the degree of neurological, motor, and functional damage caused by oral administration of $AlCl_3$. Aluminum chloride can cross the BBB, causing cognitive impairment and neuronal damage (Shunan et al., 2021). In this study, oral administration of $AlCl_3$ caused cognitive impairment and neurobehavioral deficits in the rats on days 28 and 42 (Table 2, Figs. 4 and 5). These changes were however, reversed on day 42 by HS-AuNPs treatment at doses of 5 and 10 mg/kg b.w. The findings of the present study suggest that the HS-AuNPs is site specific and could have cross the BBB to exert it therapeutic activities. This can be attributed to the small-sized AuNPs obtained in this study. Our findings is similar to the previously reported study by Singh et al.,

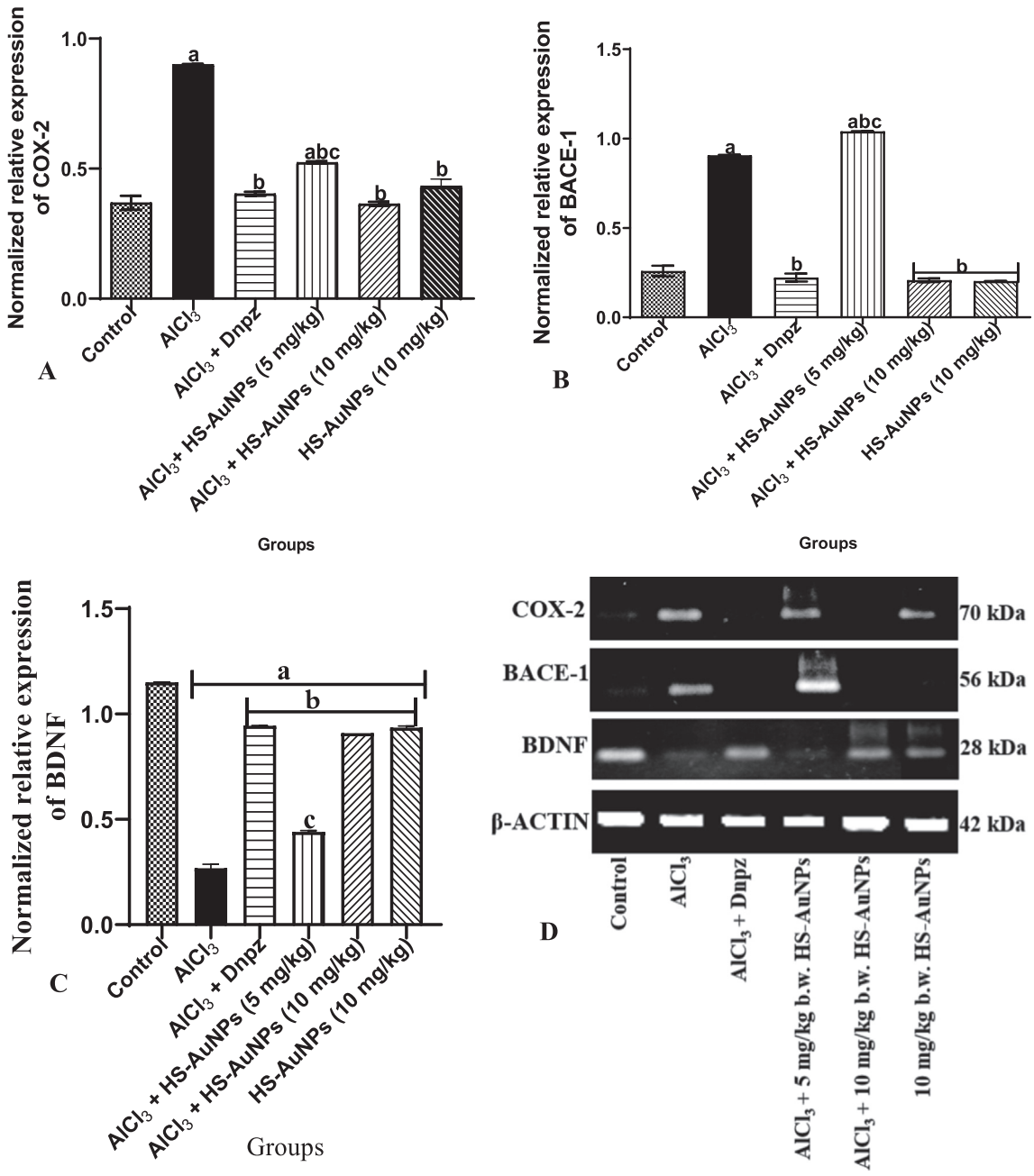

Fig. 8 Expression pattern of COX-2 (A), BACE-1 (B) BDNF (C) and pictorial representation of the band density of agarose gel electrophoresis of the RT-PCR analysis of COX-2, BACE-1, BDNF and β actin (D) genes in control, $AlCl_3$ and treatment groups. Each bar represents control normalized relative expression (gene/ β-actin). Results are expressed as mean ± SD. $^{a}p < 0.05$ vs control, $^{b}p < 0.05$ vs $AlCl_3$ group, $^{c}p < 0.05$ vs Dnpz group. Legend: $AlCl_3$ - aluminum chloride; Dnpz – donepezil; HS-AuNPs- *Hibiscus sabdariffa* synthesized-gold nanoparticles.

(2018) where nanoEGCG reversed the impaired recognition memory caused by $AlCl_3$ administration.

The significant reduction in the % weight gain of rats caused by $AlCl_3$ administration was reversed in the AD rats treated with HS-AuNPs at doses of 5 and 10 mg/kg b.w. Also, $AlCl_3$ caused an increase in the size and relative brain weight of rats, whereas the HS-AuNPs treated groups restored the relative brain weight of rats comparably to the control. The increased relative brain weight of rat observed in this study could be linked to $AlCl_3$ toxicity resulting from the long-term exposure of rats to $AlCl_3$.

Acetylcholine (ACh) is a cholinergic neurotransmitter responsible for various cognitive functions such as learning, memory, and cognition. Acetylcholinesterase is an enzyme responsible for ACh hydrolysis and a good indicator for cholinergic neuronal damage (Anadozie et al., 2019). In the present study, the elevated AChE activity caused by oral administration of $AlCl_3$ was significantly reduced by HS-

AuNPs at doses of 5 and 10 mg/kg b.w., thus, suggesting that HS-AuNPs could increase the levels of acetylcholine and promote cognitive functions. The findings of this study correlate with the previously reported study by Auti and Kulkarni (2019) where $AlCl_3$-induced rats displayed elevated AChE levels when compared to control rats.

Monoamine oxidase is a neuronal enzyme responsible for catalyzing the oxidative deamination of monoamine neurotransmitters such as norepinephrine, dopamine, and serotonin to produce peroxide (H_2O_2) (Behl et al., 2021). Previous studies have demonstrated that memory decline in an aging adult is linked to a reduced level of biogenic amine neurotransmitters in the brain (El-Baz et al., 2021, Gasiorowska et al., 2021). In the present study, $AlCl_3$ significantly increased MAO activity, which could reduce monoamine neurotransmitters levels and subsequently upsurge the generation of OS in the AD brain (Oboh et al., 2020). Treatment with HS-AuNPs at tested doses reversed this action by decreasing the activity of MAO.

Adenosine deaminase is a neuromodulator most predominant in the brain and lymphoid tissues (Sauer et al., 2017). In the central nervous system, the release of biogenic amines neurotransmitters is controlled by adenosine (Shen et al., 2018). In the present study, HS-AuNPs was able to modulate the elevated ADA activity in the brain of $AlCl_3$-induced rats.

The brain utilizes high amount of oxygen for its daily activities and therefore, most vulnerable to OS (Stefanatos and Sanz 2018). In the present study, oral administration of $AlCl_3$ increased the levels of MDA and reduced the antioxidant system (SOD, GSH and GPx) which can be linked to cognitive impairment and OS. Treatment with HS-AuNPs however, reversed the oxidative damage induced by the $AlCl_3$. Our findings correlate with the previously reported study by Shunan et al., (2021) where $AlCl_3$-induced AD was linked to an increased activity of oxidative marker and a reduction in the antioxidant systems.

The brain's functioning can be monitored by the expression of COX-2, BACE-1 and BDNF. Cyclooxygenase-2 is closely associated with neuroinflammatory disorders, and its expression is upregulated in AD (Tyagi et al., 2020). It is an early neuronal gene highly expressed in hippocampus and cortical glutamatergic neurons (Syed et al., 2015). In the present study, oral administration of $AlCl_3$ increased the mRNA expression of COX-2 in the hippocampi of the AD rats. The HS-AuNPs especially at 10 mg/kg b.w. was able to downregulate the mRNA expression of COX-2.

Beta-secretase 1 is a major target for AD therapy. Its activity in an AD patient's brain is relatively high. Also, its cleavage of APP is a rate-limiting step in Aβ production (Hampel et al., 2021). The findings of the present study showed that oral administration of $AlCl_3$ significantly upregulated the mRNA expression of BACE-1 in the hippocampi of the rats. The HS-AuNPs at 10 mg/kg b. w. however, modulated the expression of BACE-1 gene. The HS-AuNPs could have block the enzymatic cleavage of the amyloid beta precursor protein (AβPP) thereby inhibiting the expression of BACE-1. Similar observation has been reported in the study by Cai et al., (2018), where *Berberis vulgaris* extract decreased Aβ levels and inhibit the mRNA expression of BACE-1.

Brain-derived neurotrophic factor (BDNF) plays a vital role in regulating neuronal survival and neuroplasticity in the brain, as well as promoting growth, differentiation, and repair of neurons (Lin and Huang 2020). In this study, oral administration of $AlCl_3$ subsequently initiated OS by decreasing the mRNA expression of BDNF in the hippocampi of the rats. However, the AD rats treated with HS-AuNPs was able to reverse the changes in the mRNA expression of this gene. This, therefore, suggest the therapeutic role of HS-AuNPs and its ability to cross the BBB, which could be related to the size and shape of the AuNPs.

5. Conclusion

The present study evaluated the effect of HS-AuNPs on AD rats. The results of this study showed that HS-AuNPs could improve the memory and cognitive functions of $AlCl_3$-induced AD rats, as well as ameliorate the neuronal damage caused by $AlCl_3$. The 10 mg/kg HS-AuNPs was more effective than the 5 mg/kg HS-AuNPs. The therapeutic effect of HS-AuNPs could be because of its ability to penetrate the BBB and prevent the aggregation of Aβ plaque. The result of the present study suggests that HS-AuNPs could be a promising treatment approach for managing AD. The study recommends drug loading and release activities of the HS-AuNPs to further support the current study's findings.

Authors contribution

SOA conceived and designed the experiments, SOA and DOE drafted the manuscript, DOE, JIJ and IZ performed the experiment, OBA and OBA performed the data analysis, JNO and SR reviewed the manuscript, FOA and CCI All authors contributed significantly to this manuscript, read, and gave final approval of the version to be published.

Declaration of Competing Interest

The authors declare that they have no known competing financial interests or personal relationships that could have appeared to influence the work reported in this paper.

Appendix A. Supplementary material

Supplementary data to this article can be found online at https://doi.org/10.1016/j.arabjc.2023.104604.

References

Adewale, O.B., Egbeyemi, K.A., Onwuelu, J.O., et al, 2020. Biological synthesis of gold and silver nanoparticles using leaf extracts of *Crassocephalum rubens* and their comparative in vitro antioxidant activities. Heliyon 6, e05501.

Ahmed, R.H., Mustafa, D.E., 2020. Green synthesis of silver nanoparticles mediated by traditionally used medicinal plants in Sudan. Int. Nano Lett. 10, 1–14. https://doi.org/10.1007/s40089-019-00291-9.

Alía, M., Horcajo, C., Bravo, L., et al, 2003. Effect of grape antioxidant dietary fiber on the total antioxidant capacity and the activity of liver antioxidant enzymes in rats. Nutr. Res. 23, 1251–1267.

Anadozie, S.O., Akinyemi, J.A., Adewale, O.B., et al, 2019. Prevention of short-term memory impairment by *Bryophyllum pinnatum* (Lam.) Oken and its effect on acetylcholinesterase changes in CCl4-induced neurotoxicity in rats. J. Basic Clin. Physiol. Pharmacol. 30. https://doi.org/10.1515/jbcpp-2018-0161.

Anadozie, S.O., Adewale, O.B., Meyer, M., et al, 2021. *In vitro* antioxidant and cytotoxic activities of gold nanoparticles synthesized

from an aqueous extract of the *Xylopia aethiopica* fruit. Nanotechnology. https://doi.org/10.1088/1361-6528/abf6ee.

Anadozie, S.O., Adewale, O.B., Fadaka, A.O., et al, 2022. Synthesis of gold nanoparticles using extract of *Carica papaya* fruit: Evaluation of its antioxidant properties and effect on colorectal and breast cancer cells. Biocatal. Agric. Biotechnol. 42,. https://doi.org/10.1016/j.bcab.2022.102348 102348.

Antunes, M., Biala, G., 2012. The novel object recognition memory: neurobiology, test procedure, and its modifications. Cogn. Process. 13, 93–110. https://doi.org/10.1007/s10339-011-0430-z.

Auti, S.T., Kulkarni, Y.A., 2019. Neuroprotective Effect of Cardamom oil against aluminum induced neurotoxicity in rats. Front. Neurol. 10. https://doi.org/10.3389/fneur.2019.00399.

Bala, N., Saha, S., Chakraborty, M., et al, 2015. Green synthesis of zinc oxide nanoparticles using *Hibiscus subdariffa* leaf extract: effect of temperature on synthesis, anti-bacterial activity and anti-diabetic activity. RSC Adv. 5, 4993–5003.

Bawazeer, S., Rauf, A., Nawaz, T., et al, 2021. Punica granatum peel extracts mediated the green synthesis of gold nanoparticles and their detailed in vivo biological activities. Green Process. Synth, 10, 882–892. https://doi.org/10.1515/gps-2021-0080.

Bazzari, F.H., Abdallah, D.M., El-Abhar, H.S., 2019. Chenodeoxycholic acid ameliorates $AlCl_3$)-induced Alzheimer's disease neurotoxicity and cognitive deterioration via enhanced insulin signaling in rats. Molecules 24. https://doi.org/10.3390/molecules24101992.

Behl, T., Kaur, D., Sehgal, A., et al, 2021. Role of monoamine oxidase activity in alzheimer's disease: an insight into the therapeutic potential of inhibitors. Molecules 26, 3724.

Breijyeh, Z., Karaman, R., 2020. Comprehensive review on alzheimer's disease: causes and treatment. Molecules (Basel, Switzerland). 25, 5789. https://doi.org/10.3390/molecules25245789.

Cai, Z., Wang, C., He, W., et al, 2018. Berberine alleviates amyloid-beta pathology in the brain of APP/PS1 transgenic mice via inhibiting β/γ-Secretases activity and enhancing α-secretases. Curr. Alzheimer Res. 15, 1045–1052. https://doi.org/10.2174/1567205015666180702105740.

Cheignon, C., Tomas, M., Bonnefont-Rousselot, D., et al, 2018. Oxidative stress and the amyloid beta peptide in Alzheimer's disease. Redox Biol. 14, 450–464. https://doi.org/10.1016/j.redox.2017.10.014.

Conte, R., Luca, I.D., Luise, A.D., et al, 2016. New therapeutic potentials of nanosized phytomedicine. J. Nanosci. Nanotechnol. 16, 8176–8187.

Danaei, M., Dehghankhold, M., Ataei, S., et al, 2018. Impact of particle size and polydispersity index on the clinical applications of lipidic nanocarrier systems. Pharmaceutics 10, 57.

DeTure, M.A., Dickson, D.W., 2019. The neuropathological diagnosis of Alzheimer's disease. Mol. Neurodegener. 14, 32. https://doi.org/10.1186/s13024-019-0333-5.

Dong, X., 2018. Current strategies for brain drug delivery. Theranostics. 8, 1481–1493. https://doi.org/10.7150/thno.21254.

El-Baz, F.K., Abdel Jaleel, G.A., Hussein, R.A., et al, 2021. *Dunalialla salina* microalgae and its isolated zeaxanthin mitigate age-related dementia in rats: modulation of neurotransmission and amyloid-β protein. Toxicol. Rep. 8, 1899–1908. https://doi.org/10.1016/j.toxrep.2021.11.021.

ELBini-Dhouib, I., Doghri, R., Ellefi, A., et al, 2021. Curcumin attenuated neurotoxicity in sporadic animal model of Alzheimer's disease. Molecules 26, 3011.

Ellman, G.L., 1959. Tissue sulfhydryl groups. Arch. Biochem. Biophys. 82, 70–77.

Ellman, G.L., Courtney, K.D., Andres, V., et al, 1961. A new and rapid colorimetric determination of acetylcholinesterase activity. Biochem. Pharmacol. 7, 88–95. https://doi.org/10.1016/0006-2952(61)90145-9.

Gasiorowska, A., Wydrych, M., Drapich, P., et al, 2021. The Biology and pathobiology of glutamatergic, cholinergic, and dopaminergic signaling in the aging brain. Front. Aging Neurosci. 13. https://doi.org/10.3389/fnagi.2021.654931.

Giusti, G., 1974. Adenosine Deaminase. In: Bergmeyer, H.U. (Ed.), Methods of Enzymatic Analysis (second edition). Academic Press, pp. 1092–1099.

Green, A., Haughton, T.M., 1961. A colorimetric method for the estimation of monoamine oxidase. Biochem. J 78, 172.

Hampel, H., Vassar, R., De Strooper, B., et al, 2021. The β-secretase BACE1 in Alzheimer's disease. Biol. Psychiatry 89, 745–756.

He, W., Goodkind, D., Kowal, P.R., 2016. An aging world: 2015. United States Census Bureau Washington, DC.

Igbokwe, I.O., Igwenagu, E., Igbokwe, N.A., 2019. Aluminium toxicosis: a review of toxic actions and effects. Interdiscip. Toxicol. 12, 45–70. https://doi.org/10.2478/intox-2019-0007.

Izquierdo-Vega, J.A., Arteaga-Badillo, D.A., Sánchez-Gutiérrez, M., et al, 2020. Organic acids from roselle (*Hibiscus sabdariffa* L.)-A Brief review of its pharmacological effects. Biomedicines. 8, 100. https://doi.org/10.3390/biomedicines8050100.

Jalalyazdi, M., Ramezani, J., Izadi-Moud, A., et al, 2019. Effect of *Hibiscus sabdariffa* on blood pressure in patients with stage 1 hypertension. J. *Adv. Pharma. Technol. Res.* 10, 107–111. https://doi.org/10.4103/japtr.JAPTR_402_18.

Justin-Thenmozhi, A., Dhivya Bharathi, M., Kiruthika, R., et al, 2018. Attenuation of aluminum chloride-induced neuroinflammation and caspase activation through the AKT/GSK-3β pathway by hesperidin in wistar rats. Neurotox. Res. 34, 463–476.

Khan, I., Saeed, K., Khan, I., 2019. Nanoparticles: Properties, applications and toxicities. Arab. J. Chem. 12, 908–931. https://doi.org/10.1016/j.arabjc.2017.05.011.

Liaquat, L., Sadir, S., Batool, Z., et al, 2019. Acute aluminum chloride toxicity revisited: Study on DNA damage and histopathological, biochemical and neurochemical alterations in rat brain. Life Sci. 217, 202–211.

Lin, C.-C., Huang, T.-L., 2020. Brain-derived neurotrophic factor and mental disorders. Biomed. J. 43, 134–142. https://doi.org/10.1016/j.bj.2020.01.001.

Mietelska-Porowska, A., Wasik, U., Goras, M., et al, 2014. Tau protein modifications and interactions: their role in function and dysfunction. Int. J. Mol. Sci. 15, 4671–4713.

Mourdikoudis, S., Pallares, R.M., Thanh, N.T., 2018. Characterization techniques for nanoparticles: comparison and complementarity upon studying nanoparticle properties. Nanoscale 10, 12871–12934.

Nichols, E., Vos, T., 2021. The estimation of the global prevalence of dementia from 1990–2019 and forecasted prevalence through 2050: an analysis for the global burden of disease (GBD) study 2019. Alzheimers Dement. 17, e051496. https://doi.org/10.1002/alz.051496.

Oboh, G., Adedayo, B.C., Adetola, M.B., et al, 2020. Characterization and neuroprotective properties of alkaloid extract of *Vernonia amygdalina* Delile in experimental models of Alzheimer's disease. Drug Chem. Toxicol., 1–10

Ohkawa, H., Ohishi, N., Yagi, K., 1979. Assay for lipid peroxides in animal tissues by thiobarbituric acid reaction. Anal. Biochem. 95, 351–358.

Ohta, S., Kikuchi, E., Ishijima, A., et al, 2020. Investigating the optimum size of nanoparticles for their delivery into the brain assisted by focused ultrasound-induced blood-brain barrier opening. Sci. Rep. 10, 18220. https://doi.org/10.1038/s41598-020-75253-9.

Patra, J.K., Das, G., Fraceto, L.F., et al, 2018. Nano based drug delivery systems: recent developments and future prospects. J. Nanobiotechnol. 16, 71. https://doi.org/10.1186/s12951-018-0392-8.

Pellow, S., Chopin, P., File, S.E., et al, 1985. Validation of open:closed arm entries in an elevated plus-maze as a measure of anxiety in the rat. J. Neurosci. Methods 14, 149–167. https://doi.org/10.1016/0165-0270(85)90031-7.

Rajput, A., Sharma, R., Bharti, R., 2022. Pharmacological activities and toxicities of alkaloids on human health. Mater. Today:. Proc. 48, 1407–1415. https://doi.org/10.1016/j.matpr.2021.09.189.

Riaz, G., Chopra, R., 2018. A review on phytochemistry and therapeutic uses of *Hibiscus sabdariffa* L. Biomed. Pharmacother. 102, 575–586.

Roy, A., 2018. Role of medicinal plants against Alzheimer's disease. Int. J. Complement. Altern. Med. 11, 205–208.

Ruangritchankul, S., Chantharit, P., Srisuma, S., et al, 2021. Adverse drug reactions of acetylcholinesterase inhibitors in older people living with dementia: a comprehensive literature review. Ther. Clin. Risk Manag. 17, 927.

Saraiva, C., Praça, C., Ferreira, R., et al, 2016. Nanoparticle-mediated brain drug delivery: Overcoming blood–brain barrier to treat neurodegenerative diseases. J. Control. Release 235, 34–47. https://doi.org/10.1016/j.jconrel.2016.05.044.

Sauer, A.V., Hernandez, R.J., Fumagalli, F., et al, 2017. Alterations in the brain adenosine metabolism cause behavioral and neurological impairment in ADA-deficient mice and patients. Sci. Rep. 7, 40136. https://doi.org/10.1038/srep40136.

Shen, H.-Y., Huang, N., Reemmer, J., et al, 2018. Adenosine actions on oligodendroglia and myelination in autism spectrum disorder. Front. Cell. Neurosci. 12. https://doi.org/10.3389/fncel.2018.00482.

Shunan, D., Yu, M., Guan, H., et al, 2021. Neuroprotective effect of Betalain against $AlCl_3$-induced Alzheimer's disease in Sprague Dawley rats via putative modulation of oxidative stress and nuclear factor kappa B (NF-κB) signaling pathway. Biomed. Pharmacother. 137,. https://doi.org/10.1016/j.biopha.2021.111369 111369.

Singh, N.A., Bhardwaj, V., Ravi, C., et al, 2018. EGCG nanoparticles attenuate aluminum chloride induced neurobehavioral deficits, beta amyloid and tau pathology in a rat Model of Alzheimer's disease. Front. Aging Neurosci. 10. https://doi.org/10.3389/fnagi.2018.00244.

Singh, J., Dutta, T., Kim, K.-H., et al, 2018. 'Green' synthesis of metals and their oxide nanoparticles: applications for environmental remediation. J. Nanobiotechnol. 16, 84. https://doi.org/10.1186/s12951-018-0408-4.

Sinha, D., 2019. Pharmacological importance of polyphenols: a review. Int. Res. J. Pharm. 10, 13–23.

Stefanatos, R., Sanz, A., 2018. The role of mitochondrial ROS in the aging brain. FEBS Lett. 592, 743–758.

Syed, H., Ikram, M.F., Yaqinuddin, A., et al, 2015. Cyclooxygenase I and II inhibitors distinctly enhance hippocampal-and cortex-dependent cognitive functions in mice. Mol. Med. Rep. 12, 7649–7656.

Tyagi, A., Kamal, M.A., Poddar, N.K., 2020. Integrated pathways of COX-2 and mTOR: roles in cell sensing and Alzheimer's disease. Front. Neurosci. 14. https://doi.org/10.3389/fnins.2020.00693.

Wendel, A., 1981. [44] Glutathione peroxidase. Methods Enzymol. *Elsevier* 77, 325–333.

Yusni, Y., Meutia, F., 2020. Action mechanism of rosella (*Hibiscus sabdariffa* L.) used to treat metabolic syndrome in elderly women. *Evid.-Based Complement*. Altern. Med. 2020, 5351318 https://doi.org/10.1155/2020/5351318.

Zangeneh, M.M., Zangeneh, A., 2020. Novel green synthesis of *Hibiscus sabdariffa* flower extract conjugated gold nanoparticles with excellent anti-acute myeloid leukemia effect in comparison to daunorubicin in a leukemic rodent model. Appl. Organomet. Chem. 34, e5271.

Zhao, Y., Zhao, B., 2013. Oxidative stress and the pathogenesis of Alzheimer's disease. Oxid. Med. Cell. Longev. 2013,. https://doi.org/10.1155/2013/316523 316523.